

A NEW OTR BASED BEAM EMITTANCE MONITOR FOR THE LINAC OF LURE

M.-A. Tordeux, J. Papadacci

Laboratoire LURE, Centre Universitaire Paris-Sud, BP 34, 91898 Orsay, France

Abstract

An electron beam emittance diagnostic has been designed and built at the Linear Accelerator of Orsay, injector of Super-ACO and DCI Storage Rings. It is based on the Optical Transition Radiation produced at the interface of a 15 μm aluminium foil, which is located in the beam path. Measurement of the energy, divergence and transverse profiles of the beam can be done in a single shot, thanks to two cooled cameras. 1D and 2D methods for fitting the data are used. Emittance measurement results for a 10 nC beam at 25 Hz and 200 MeV are given, and then compared with those obtained with the "three gradients" method. We conclude that the 1D method, although attractive, is incompatible with a precision better than 100 %.

1 INTRODUCTION

First demonstration of application of Optical Transition Radiation theory was achieved by L. Wartsky [1] on Orsay Linac. Some other experiments [2,3,4] have shown that OTR is widely usable for monitoring. Transition radiation is produced when a charged particle crosses the interface of two media with different dielectric constants, in both backward and forward directions. Since April 2000, a complete set-up allows us to make use of the backward Optical TR emitted at an aluminium foil located in the 200 MeV beam. We intend to improve the emittance measurement of the e- beam, and also point out the critical aspects of the experiment.

2 PRINCIPE

2.1 Theoretical background

In case of Lorenz factor $\gamma \gg 1$, the OTR pattern produced at the foil interface takes the shape of a very narrow cone around the specular reflection angle. Then, the following expression for OTR intensity per unit frequency and per steradian is retained [5], including the slight asymmetry when the sign of θ is changed :

$$I_{//} = \frac{e^2 \beta^2}{c \pi^2} \left\{ \frac{|r_{//}|^2 \theta^2}{(\gamma^{-2} + \theta^2)^2} + \frac{\text{Re}(r_{//}) \theta}{\gamma^{-2} + \theta^2} \right\} \quad \{1\}$$

$$I_{\perp} = \frac{e^2 \beta_{\perp}^2}{c \pi^2} \left\{ \frac{|r_{\perp}|^2}{(\gamma^{-2} + \theta^2)^2} + \frac{\text{Re}(r_{\perp})}{\gamma^{-2} + \theta^2} \right\}$$

where θ is the angle with respect to the normal of the interface, $r_{//}$ and r_{\perp} are the complex Fresnel reflection coefficients for each polarisation component, β is the particle velocity normalised to that of light, and β_{\perp} the

component of β which is perpendicular to the plane of observation.

To take in account the real electron beam with angular divergence distributions in the two transverse planes, two levels of calculation are possible. The usual one [2,3,5] proposes a 1D convolution for each polarisation {2}, assuming that a polariser will be inserted for data acquisition. Otherwise, a 2D convolution following {3} is performed, with σ_x and σ_y being the standard deviations for e- angular divergences. Intensity in a simplified expression is summed over these distributions, due to an incoherent source.

$$I(\theta_x, \theta_y) = K \iint \left(\frac{\theta}{\gamma^{-2} + \theta^2} \right)^2 \exp \left(- \frac{\alpha_x^2}{2\sigma_x^2} - \frac{\alpha_y^2}{2\sigma_y^2} \right) d\alpha_x d\alpha_y \quad \{3\}$$

where K is a normalisation constant, θ_x and θ_y the projections of the observation angle θ such that :

$$\theta^2 = (\theta_x - \alpha_x)^2 + (\theta_y - \alpha_y)^2$$

2.2 Diffraction calculation

Two aspects in the OTR emission lead to a good comprehension of the diffraction calculation. First, despite a peaked emission at $\pm \gamma^{-1}$, a large tail with a θ^2 variation ensures that no catastrophic effect from diffraction is foreseen, as shown by some experiments [6]. Secondly, the *radial* configuration of the polarisation leads to a diffraction pattern which cancels at its centre [7]. As a matter of fact, taking the simplified expression of the OTR, the classical formula for Fraunhofer diffraction amplitude can be projected for each component of the electric field. Let be $x = \rho/\lambda\gamma$ the radius in the source plane normalised to the energy and wave length, $r = \theta\gamma$ the normalised radius in a re-focussing lens and φ the azimuthal angle. We can write :

$$\vec{A}(x) = C \int_{\Sigma_{pupil}} \frac{\vec{r}}{1+r^2} e^{2i\pi \vec{x} \cdot \vec{r}} ds$$

$$\Rightarrow \begin{cases} A_{//}(x) = C \int_{r=0}^{R_{max}} \int_{\varphi=0}^{2\pi} \frac{r \cos \varphi}{1+r^2} e^{2i\pi x r \cos \varphi} r dr d\varphi \\ A_{\perp}(x) = C \int_{r=0}^{R_{max}} \int_{\varphi=0}^{2\pi} \frac{r \sin \varphi}{1+r^2} e^{2i\pi x r \cos \varphi} r dr d\varphi \end{cases}$$

$$\text{Finally, } A(x) = A_{//}(x) = 2i\pi C \int_{r=0}^{R_{max}} \frac{r^2}{1+r^2} J_1(2i\pi x r) dr$$

where J_1 is the first Bessel function, C a normalisation constant. Fig. 1 shows the amplitude module of the diffraction pattern at source point compared to the Airy disk, in the case of a total lens aperture : $\theta_{max} = 2 \cdot (5 \cdot \gamma^{-1})$.

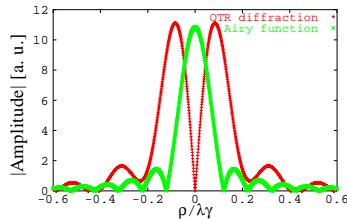


Figure 1: OTR diffraction compared to Airy function with total lens aperture $\theta_{max} = 2 \times (5 \times \gamma^{-1})$

3 EXPERIMENTAL SET-UP

3.1 Linac specifications

The Electron Accelerator of Orsay is used as well as source of positrons and also for various physics experiments. Two guns are available for injection. In our experiment, we used the one which delivers high current, using a beam transfer line. In that way, no thermal ray produced by the cathode can be collected through the optical line. Beam parameters are shown in Table 1.

Table 1: Beam Parameters

Microbunch, Macropulse Length	10 – 15 ps, 5 ns
Microbunch, Macropulse frequency	3 GHz, 25 Hz
Nb of Bunches / Macropulse	15
Charge	From 0.5 to 1 nC/Bunch
Average Energy	200 MeV

3.2 Optical device, alignment and calibration

A plate holding up two successive 15 μm aluminium foils, is movable in a vacuum chamber, with an inclination angle of 45°. In order to minimise reflections, the exit tube of the chamber is Ni plated, taking care that no Zn has been included. Another tube is mounted on the opposite side, for laser alignment. As one of the foils has been pierced with regular holes, one performs also calibration in the image plane.

The optical line shown in Fig. 2 fulfils the three following requirements :

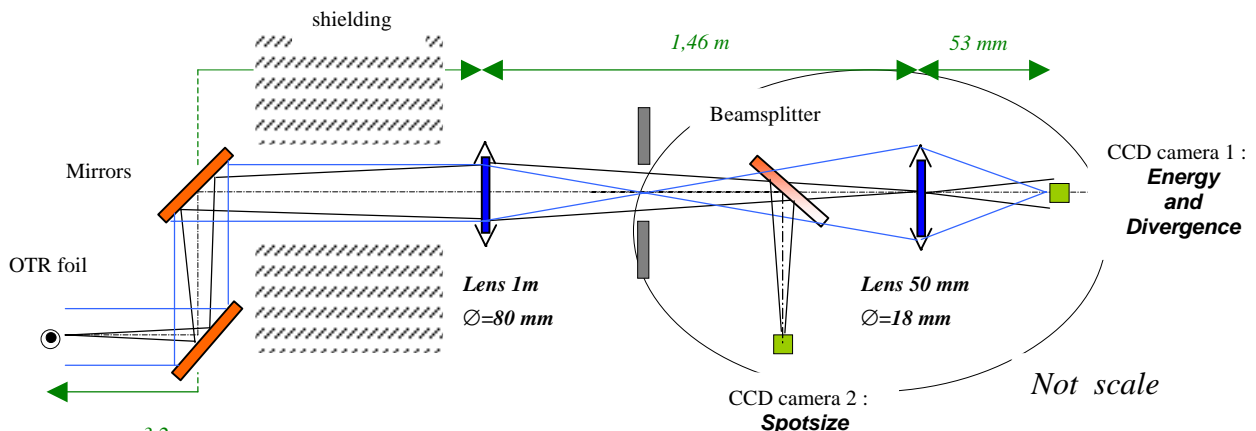


Figure 2: Layout of the optical system.

- CCD cameras and lenses are located far from the ionizing radiation (10 rem/h in operation)
- A compromise has been found for the aperture of the line : on the one hand, the inclination of the foil requires a 10 mm depth of field, but on the other hand, diffraction contribution of OTR (cf. 2.2) doesn't exceed a tenth of the typical size of the beam, that is 100 μm .
- A pollution of the low level focal plane image by the spot flux is avoided.

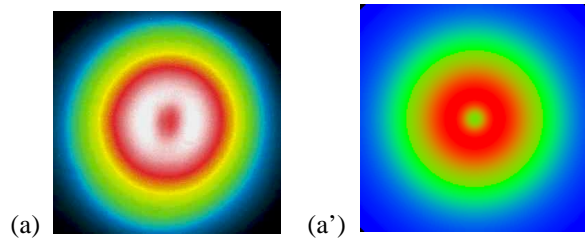
3.3 Data processing

Both cooled cameras, equipped with KAF-401E CCD acquire data during 125 ms in the image plane, up to 1 second in the focal plane. Background has been systematically subtracted from data, that is image without beam and with the same acquisition time. Unfortunately, no correction with flatfield has been possible, so dust is visible. Finally, we correct the ghost appeared on the CCD 2, due to the beamsplitter.

4 RESULTS

4.1 General features

Figure 3 shows how the 2D aspect of the OTR emission influences the pattern shape : relative intensity goes down in one direction, without insertion of any polariser. Calculation done according [3] proves that different e-angular divergences in the horizontal and vertical plane lead to such a pattern. Rotation of the figure (b) is due to non parallelism of the mirrors.



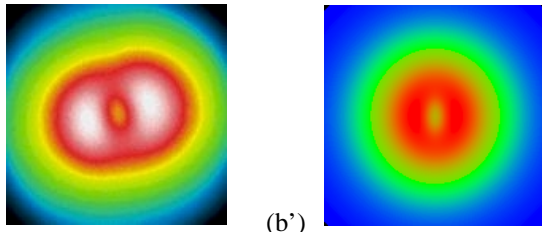


Figure 3 : OTR pattern in the focal plane. (a) measured and (a') calculated for same e- angular divergence in horizontal and vertical planes $\theta_x = \theta_y = 0.6$ mrad , $\gamma = 382$. (b) and (b') for different e- angular divergences $\theta_x = 0.4$ mrad and $\theta_y = 1.3$ mrad.

4.2 Energy measurement

We fit the OTR pattern shaped in the focal plane through a polariser, with the 1D calculation [2] and deduce average energy of the e- beam (figure 4). Because no bending magnet was available close to the device, different energy tests were performed : measurement of incident RF power in accelerating sections, of a 600 MeV e- beam in the Super-ACO transport line, variation of RF phase in the last section (figure 5). In all cases, accuracy was found to be better than 5 %.

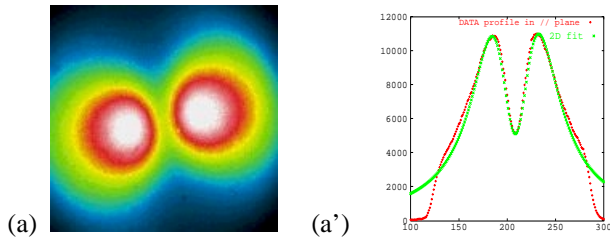


Figure 4 : (a) parallel polarised OTR pattern measured in the focal plane (a') profile fitted with 1D convolution

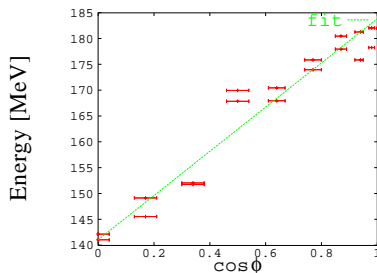


Figure 5: Measurement of beam energy versus $\cos\phi$, with ϕ the phase of RF wave in last accelerating section.

4.2 Emittance measurement

Beam transverse emittance is given by the following expression [8] : $\epsilon_{rms} = \beta\gamma \sqrt{\langle x_i^2 \rangle \langle x_i'^2 \rangle - \langle x_i x_i' \rangle^2}$, where $\langle x_i^2 \rangle$, $\langle x_i'^2 \rangle$ and $\langle x_i x_i' \rangle$ are the 2nd order moments of the distributions in position and angle.

As no measurement of $\langle x_i x_i' \rangle$ seems to be possible, we have to achieve a waist on the OTR foil. Under these conditions, we fit the OTR pattern in the focal plane with the 2D calculation [3], measure the transverse sizes of the beam, and compute the emittance in the two planes. Table

2 compares the results for a 10 nC @ 25 Hz beam with those obtained with the “three gradients method” at the same location. We also put the emittance obtained with the classical 1D convolution.

Table 2: Comparison of transverse emittance for a 10 nC @ 25 Hz beam measured with three different methods

Method	ϵ_{rms}^H	ϵ_{rms}^V
	(π mm.mrad)	(π mm.mrad)
“3 gradients”	185	96
OTR	2D conv.	105
	1D conv.	316

As expected, the beam experimented an emittance growth in the horizontal plane, due to the transfer line at 20 MeV which contains hexapole magnets.

We put all our attention into achieving a waist in the vertical plane. So, the horizontal waist was probably not correctly set, and may explain the 60 % discrepancy between the 2D convolution and 3 gradients methods.

The 1D convolution method gives an intolerable over-estimation of ϵ_{rms} as seen elsewhere. Analysis of 2D phenomena shows that contribution of one plane into the other, in filling-up the cone of emission can't be neglected, especially when the e- angular spreads are very different.

5 CONCLUSION

We are shown that the 1D treatment of OTR pattern may lead to serious errors in emittance measurement when angular divergences in horizontal and vertical plane are very different, whereas 2D treatment proves to be an interesting method. However, achieving a waist on the OTR foil remains somehow problematic, and at least time consuming. We will try to cure this point in the future.

ACKNOWLEDGEMENTS

We are greatly indebted to P. Prout, L. Vatrinet, C. Prevost and its crew, D. Betaille and the operation team of the Linac for their technical study and support. We also appreciated the helpful and stimulating discussions with F. Polack and G. Flynn.

REFERENCES

- [1] L. Wartsky et al., J. Appl. Phys. 46,3644 (1975)
- [2] D.W. Rule, TR diagnostics for intense charged particle beams, NIM B24/25 (1987) 901-904
- [3] C. Couillaud et al., Electron beam emittance measurement using OTR interferometry, EPAC 96
- [4] S. Schaeffer, Central Bureau for Nuclear Meas., Geel, Belgium, private communication
- [5] M. J. de Loos and al, Characterisation of the 50 MeV ALS Linac Beam with OTR, EPAC 96
- [6] Experimental investigations on geometrical resolution of electron beam profiles given by OTR in the GeV energy range, X. Artru and al, EPAC 1996.
- [7] F. Polack, LURE, private communication.
- [8] P. M. Lapostolle, IEEE Trans. Nucl. Sci. NS-18, N°3, 1101 (1971).